out number $n = 1650$ at $T = 0°K$,[15] one finds at the wipe-out distance of about 20 Å a charge-density oscillation amplitude which amounts to 80% of the value calculated[11] using Friedel's asymptotic expression with the resonance at the Fermi energy, i.e., $\delta_l(0) = \pi/2$, corresponding to the unitarity limit. (This large value of the first-order quadrupole wipe-out number can be understood only if d-wave scattering dominates over the s- and p-type scattering, in accordance with our previous assumption.) Looking now at Fig. 1, we see that in this case ξ_Δ cannot be greater than approximately half of the above radius, i.e., $\xi_\Delta \leq 10$ Å, which means that $\Delta \geq 0.5$ eV, a value close to the width of the vbs in Al-based alloys of about 0.6 eV,[13] and an order of magnitude larger than $k_B T_K$. This fact rules out the existence of a single narrow Kondo resonance, and so we are forced to assume that in the temperature dependence of the different macroscopic properties and of the charge density oscillation,[14] the temperature dependence of the scattering amplitude $t_l(0)$ plays a major role, and/or that $t_l(\omega)$ has a much more complex structure than that corresponding to a single-peaked conventional resonance, in which case our considerations have to be applied with particular care.[16]

The analysis shows the fundamental importance of determining the charge-density oscillation in the nonmagnetic regime (below T_K) of "typical" Kondo systems. Thus, we propose first of all the experimental determination of the amplitude of the charge density oscillation in the $T \to 0°K$ limit, as measured by the first-order NMR quadrupole effect, in the *Cu*Fe and *Cu*Co alloy systems. An analysis of the results along the present lines would provide a crucial test of the existence of a Kondo-type resonance in these alloys.

The authors are indebted to C. Berthier and M. Minier for making their data available before publication, and to C. Hargitai and A. Zawadowski for valuable discussions.

*Present address: Institute Laue-Langevin, Grenoble, France.

†Present address: Imperial College, Department of Physics, London, England.

[1]J. Friedel, Can. J. Phys. 34, 1190 (1956).

[2]L. C. R. Alfred and D. O. van Ostenburg, Phys. Lett. 26A, 27 (1967).

[3]Y. Fukai and K. Watanabe, Phys. Rev. B 2, 2353 (1970); K. Tompa, in Conference on the Electric and Magnetic Properties of dilute Alloys, Tihany, 1971 (unpublished).

[4]T. J. Rowland, Phys. Rev. 119, 900 (1960).

[5]C. Berthier and M. Minier, to be published.

[6]M. Minier, Phys. Rev. 182, 437 (1969).

[7]F. Mezei and A. Zawadowski, Phys. Rev. B 3, 167 (1971).

[8]*Handbook of Mathematical Functions with Formulas, Graphs, and Mathematical Tables*, edited by M. Abramowitz and I. A. Stegun (Dover, New York, 1965).

[9]D. R. Hamann, Phys. Rev. 158, 570 (1967).

[10]I. Adawi, Phys. Rev. 146, 379 (1966).

[11]G. Grüner and F. Mezei, to be published.

[12]J. Kondo, in *Solid State Physics*, edited by F. Seitz and T. Turnbull (Academic, New York, 1969), Vol. 23.

[13]E.g., W. M. Star, thesis, University of Leiden, 1971 (unpublished).

[14]A. D. Caplin and C. Rizzuto, Phys. Rev. Lett. 21, 746 (1968).

[15]G. Grüner and C. Hargitai, Phys. Rev. Lett. 26, 772 (1971), and to be published.

[16]G. Grüner and A. Zawadowski, Solid State Commun. 11, 663 (1972).

Magnetic Structures of Samarium*

W. C. Koehler and R. M. Moon

Solid State Division, Oak Ridge National Laboratory, Oak Ridge, Tennessee 37830

(Received 10 October 1972)

The magnetic structures of metallic samarium have been determined from neutron-diffraction data on a single crystal of ^{154}Sm. Anomalies in a number of physical properties of this metal at 106 and 13.8°K are associated with ordering of the moments on the hexagonal and cubic sites, respectively. The unusual form factor expected for a $4f^5$ configuration has been observed. Striking evidence for important conduction-electron polarization effects has been found.

Anomalies in the electrical resistivity[1] and specific heat[2,3] of samarium have been detected near 106 and 14°K, which are suggestive of magnetic-ordering transitions at these temperatures. Recently, single-crystal magnetic-susceptibility data have been reported,[4] which are explicable if Sm at 4.2°K is a c-axis antiferromagnet. Up until now, neutron-diffraction studies of this metal

have not been attempted because of the prohibitively high thermal-neutron capture cross section of the naturally occurring element. We have recently obtained[5] a large single crystal of Sm highly enriched in the relatively low-capturing isotope ^{154}Sm ($\sigma \approx 60$ b). It is the purpose of this note to describe briefly the results of neutron scattering experiments carried out with this crystal; a complete account is in preparation.

As matters developed, the large single crystal was essential for a successful magnetic-structure determination. Because of the complexity of the magnetic structures, and of the low ordered moments, the magnetic intensities in a powder pattern, even with the isotopic sample, could not have been resolved from the nuclear reflections.

The complexity of the magnetic structures is due in part to the fact that the crystal structure of Sm is somewhat complicated.[6] It is rhombohedral, space group $R\bar{3}m$ with three atoms per unit cell. The structure can be envisaged, however, as a nine-layer stacking sequence, *ABAB-CBCAC*$\cdots$, of close-packed hexagonal layers. (Actually, there are two coexisting structural domains in any metal specimen which differ from each other by a rotation of 180° about the normal to the layers, the *c* axis. The second domain has the sequence *ACACBCBAB*$\cdots$.) Two thirds of the atoms have near-neighbor layer configurations similar to that found in the simple hexagonal structure, *ABAB*$\cdots$ stacking, and one third similar to that of cubic close packing, *ABCAB-C*$\cdots$ stacking. It will be convenient in the following to refer to these as hexagonal and cubic sites, respectively, even though the site symmetries are not exactly those of the ideal hexagonal and cubic close packing.

Metallic samarium is assumed to consist of tripositive ions in a sea of conduction electrons. The $4f^5$ configuration characteristic of Sm^{+3} can give rise to some extremely interesting spectroscopic and magnetic properties. In the fully ordered free-ion ground state $^6H_{5/2}$ ($L=5$, $S=\frac{5}{2}$, $J=\frac{5}{2}$, $J_z=\frac{5}{2}$) the spin and orbital contributions to the total moment are opposed and they produce an ordered moment gJ equal to $\frac{5}{7}\mu_B$. This partial cancelation of spin and orbital moment will, as well, produce an unusual form factor, namely, one that peaks at a value of $\sin(\theta)/\lambda$ which is not zero. The actual ground state may be different from the free-ion ground state as a result of crystal-field splittings of the lowest-lying multiplet, and of admixture to the ground multiplet from a low-lying excited $^6H_{7/2}$ multiplet. The magnitude of the moment and the shape of the form factor can be quite sensitive to the exact nature of the ground state. The effect of conduction-electron polarization, recognized as a small but definite contribution to the magnetization of the heavy rare-earth metals, can be relatively much more important in the case of Sm. Indeed, we believe that we have striking experimental evidence for a contribution to the total moment of Sm from conduction-electron polarization which, in magnitude, is of the same order as that from the $4f$ electrons.

Neutron-diffraction data were collected at room temperature to establish the crystallographic domain populations. For the magnetic structure studies, not having powder data to use as a guide, it was necessary to carry out a long series of search scans. Below 106°K, magnetic reflections were found on reciprocal lattice rows parallel to the reciprocal *c*-axis $\vec{b}_3$. One pair of reflections was associated with each allowed nuclear reflection, except for reflections (00*l*), and separated by $\pm 1.5\vec{b}_3$ from it. The high-temperature magnetic structure which we have deduced from the data is shown in Fig. 1(a). Each plane of hexagonal sites froms a ferromagnetic sheet with the moments in the sheet parallel to the *c* axis. This series of ferromagnetic sheets has the sequence $0++0--0++\cdots$ along the *c* axis as shown. The zeros represent the cubic-site planes, the moments on which are disordered.[7] The *c* axis of the high-temperature magnetic unit cell is twice as long as that of the chemical unit cell. This structure has the interesting property that it produces an exchange interaction which exactly vanishes at the cubic sites, thus providing a nice self-consistency check on the model.

Below 13.8°K additional magnetic reflections were observed which require that the *c* axis and one of the hexagonal *a* axes of the chemical cell be quadrupled. The magnetic reflections characteristic of the low-temperature structure fall on two sets of lines in the $h0l$ section of the reciprocal lattice for which the magnetic-cell indices satisfy $l+h=12n$ or $l-h=12n$ with n equal to an integer. Each set of lines is associated with one structural domain. Since each of the chemical-cell *a* axes is a possible unique magnetic-cell parameter, there are in all six magnetic domains. The intensities of reflections due to the high-temperature structure show no change as the sample temperature is reduced below 13.8°K. Therefore, we conclude that the lower transition temperature is a magnetic-ordering transition for the moments

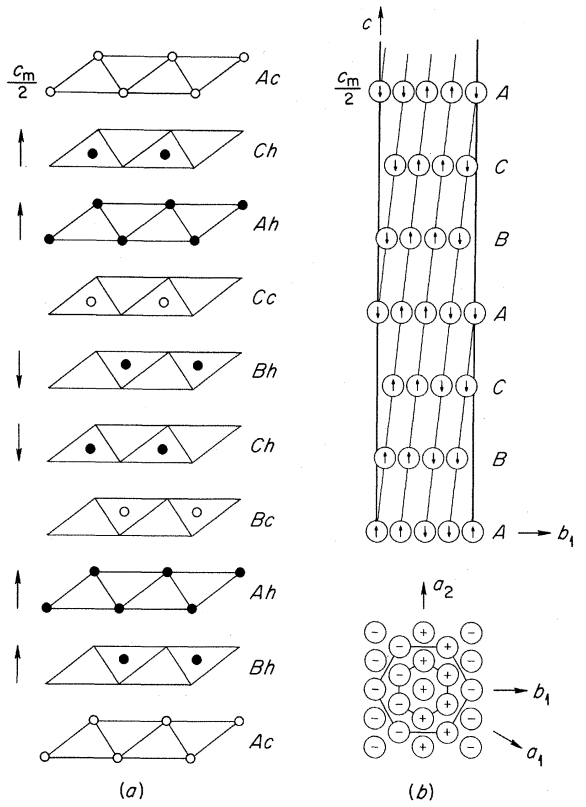

FIG. 1. (a) High-temperature magnetic structure involving only the hexagonal-site ions. Closed circles, hexagonal sites (*h*); open circles, cubic sites (*c*). The hexagonal sites are coupled ferromagnetically within layers normal to the *c* axis. The moment direction within each layer is indicated by the arrows. Only half of the magnetic unit cell is shown. The upper half is the same as the lower half, but with all moments reversed. (b) Low-temperature magnetic structure involving only cubic-site ions. In the lower part is shown the antiferromagnetic structure within a single layer with nearest- and next-nearest-neighbor coordination emphasized. In the upper part is shown a projection of the magnetic unit cell onto the plane containing $\vec{c}$ and $\vec{b}_1$. The arrows stand for rows of atoms along the $\vec{a}_2$ direction with moments directed along the arrows. The layers containing hexagonal sites are not shown. Only half of the magnetic cell is shown. The upper half is generated by translating the lower half by $\vec{c}_M/2$ and reversing the direction of all moments.

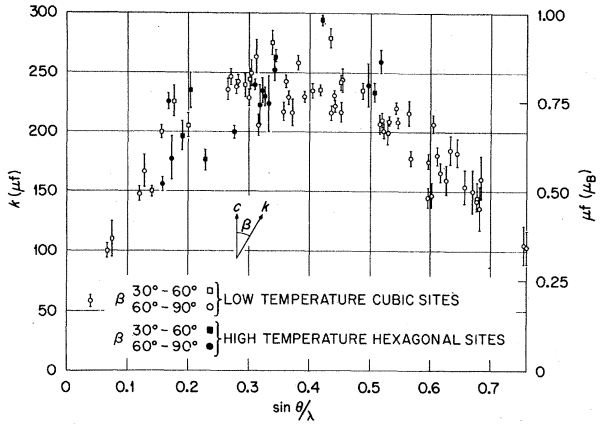

FIG. 2. Magnetic scattering amplitudes observed in metallic Sm. The angular ranges corresponding to different symbols refer to β, the angle between $\vec{c}$ and the scattering vector.

on the cubic sites.

A magnetic structure which accounts for the observations is shown in Fig. 1(b). Subject to several reasonable assumptions (collinear moments, no interaction with the hexagonal sites), this structure can be shown to be uniquely determined by the observed positions of the magnetic peaks.

An important element to consider in the cubic-site ordering is the fact that the adjacent cubic layers are almost 9 Å apart; thus the dominant exchange interactions are those occurring in the same layer. Therefore, we first describe the structure in a single layer perpendicular to the *c* axis and then describe how these layers are coupled together. The single-layer structure is shown at the bottom of Fig. 1(b). It consists of ferromagnetic rows parallel to the hexagonal $\vec{a}_2$ axis, with a $++--\cdots$ sequence along the $\vec{a}_1$ axis. The ferromagnetic rows are thus perpendicular to the reciprocal $\vec{b}_1$ axis. At the top of Fig. 1(b), we show how the ferromagnetic rows are coupled along the $\vec{c}$ direction to form ferromagnetic sheets parallel to $(\bar{1}01)$ planes. The stacking sequence along the normal to these sheets is $++--\cdots$. The resulting magnetic cell has dimensions of 103.6 Å along $\vec{c}$, 14.51 Å along $\vec{a}_1$, and 3.63 Å along $\vec{a}_2$. As in the high-temperature structure, the moments are parallel to the $\vec{c}$ axis.

The observed magnetic intensities have been reduced to quantities proportional to the magnetic scattering amplitudes per atom, and these are shown as a function of $\sin(\theta)/\lambda$ in Fig. 2. In a separate experiment on powdered SmN, the nuclear scattering amplitude of the isotopic mixture of our sample was determined. This allowed the amplitudes of Fig. 2 to be placed on an absolute basis, as shown on the right-hand scale. A detailed report on the interpretation of these amplitudes is in preparation. For the present, we make only a few qualitative remarks. The most striking feature of the data is the rapid decrease observed as $\sin(\theta)/\lambda$ approaches zero. The extrapolation of these data to $\sin(\theta)/\lambda = 0$ would give

the net moment per atom. We are uncertain about how to make this extrapolation, but surely the net moment is quite small, probably close to $0.1\mu_B$. We believe that the free-ion moment of $0.71\mu_B$ is partly reduced by crystal-field effects and that there is a large polarization of the conduction electrons parallel to the ionic spin. The combination of ionic plus conduction spin moment almost cancels the orbital moment which is directed in the opposite sense. The radial dependences of the total spin and the orbital moment densities are quite different, so that the net moment is not small everywhere. There are regions of positive and negative magnetization which nearly average to zero when integrated over an ionic volume. These results concur with those of a recent calculation by Stewart[8] who has shown that the influence of conduction-electron polarization effects upon the susceptibilities of metals containing tripositive samarium ions is very much greater than those of metals containing the heavy rare earths. His application of the theory to metallic samarium itself, however, must be modified because he assumed all the Sm ions to be paramagnetic above 15°K.

From our knowledge of the existing structures we can draw some interesting conclusions about the radial dependence of the exchange interaction in a simple isotropic exchange theory. We assume that the exchange energy is given by

$$E_{ex} = -\sum_{i \neq j} J(r_{ij}) \vec{S}_i \cdot \vec{S}_j . \quad (1)$$

Consider first the cubic-site structure where we expect the dominant interactions to be those involving ions in the same basal plane. There are six nearest neighbors at a distance a and six more at $\sqrt{3}a$, as shown in Fig. 1(b). This latter group is actually a part of the fourth-neighbor group in the three-dimensional structure. If we consider only these two contributions to the sum in Eq. (1), then it is a simple matter to write down the single-site exchange energies for various single-layer structures. We define an "*a*" antiferromagnet as one with ferromagnetic rows parallel to an $\vec{a}$ axis and designate the particular structure by giving the stacking sequence normal to this direction. Similarly a "*b*" antiferromagnet has ferromagnetic rows along a reciprocal-lattice $\vec{b}$ axis. The single-site exchange energies for the four most obvious structures[9] are given in Table I. The observed structure corresponds to the first entry in the table. By inspection, we conclude that $J_1 > 0$ is a necessary condition for stabilization of the observed structure against all of the other antiferromagnetic arrangements. For the observed structure to have a lower energy than the ferromagnet, we require that $-J_4/J_1 > \frac{1}{2}$. We conclude that within a single layer, the nearest-neighbor interaction is ferromagnetic and the next-nearest interaction is antiferromagnetic and of comparable magnitude. Perhaps the sum should be carried to further neighbors, but it seems that the essential features are contained in the above discussion. These conclusions are consistent with the general picture of indirect exchange via polarization of the conduction electrons as contained in the Ruderman-Kittel-Kasuya-Yosida (RKKY) theory.

TABLE I. Comparison of exchange energies associated with various single-layer magnetic structures.

Type	Structure	E_{ex}/S^2
a	++−−	$-2J_1+2J_4$
a	+−+−	$2J_1+2J_4$
b	++−−	$2J_1+2J_4$
Ferro	++++	$-6J_1-6J_4$

The situation is more complex when considering the stability of the hexagonal-site structure. Contributions from ions displaced one and two layers along the c axis must be considered if all interactions out to fourth neighbors are included. We find that the observed structure is consistent with exchange interactions such as $J_1 > J_2 > 0 > J_3 > J_4$. Again, these are reasonable conditions from the viewpoint of the RKKY theory.

*Research sponsored by the U. S. Atomic Energy Commision under contract with the Union Carbide Corporation.

[1]S. Arajs and G. R. Dunmyre, Z. Naturforsch. 21 1856 (1966).

[2]L. M. Roberts, J. Phys. B: Proc. Phys. Soc., London 70, 343 (1957).

[3]L. D. Jennings, E. D. Hill, and F. H. Spedding, J. Chem. Phys. 31, 1240 (1959).

[4]S. Foner, C. Voight, and E. J. Alexander, in *Magnetism and Magnetic Materials—1972,* AIP Conference Proceedings No. 5, edited by C. D. Graham, Jr., and J. J. Rhyne (American Institute of Physics, New York, 1972), p. 1435.

[5]R. E. Reed, in *Proceedings of the Ninth Rare-Earth Research Conference, Blacksburg, Virginia, 1971,* edited by P. E. Field (Virginia Polytechic Institute Press, Blacksburg, Va., 1971), p. 657.

[6]A. H. Daane, R. E. Rundle, H. G. Smith, and F. H. Spedding, Acta Crystallogr. 7, 532 (1954).

[7]This structure can also be considered as an oscillatory structure so phased as to have zero moment at the cubic sites.

[8]A. M. Stewart, Phys. Rev. B 6, 1985 (1972).

[9]The four structures listed have been shown to be the only possible configurations which satisfy a physically reasonable constraint. H. A. Gersch and W. C. Koehler, J. Phys. Chem. Solids 5, 180 (1958). In their notation the structures are $(\pi/2,\bar{\pi}/2)$, (π,π), $(\pi/2,\pi/2)$, and (0, 0), respectively.

Decay of the Lowest $T=2$ State in ^{44}Ti

J. J. Simpson
University of Guelph, Guelph, Canada

and

W. R. Dixon and R. S. Storey
National Research Council of Canada, Ottawa, Canada
(Received 21 September 1972)

The lowest $T=2$ state in ^{44}Ti has been found in the reaction ^{40}Ca$(\alpha,\gamma)^{44}$Ti at an excitation energy of 9338 ± 2 keV in ^{44}Ti. The radiative yield has been measured and the γ decay has been studied.

The lowest $T=2$ state in ^{44}Ti has previously been located by use of the reaction[1-3] ^{46}Ti$(p, t)^{44}$Ti. The most recent determination,[3] having the smallest assigned energy uncertainty, gives an excitation energy of 9330 ± 10 keV. We wish to report the γ decay of this state studied by using the reaction ^{40}Ca$(\alpha,\gamma)^{44}$Ti.

A 10–15-μA beam of doubly charged helium ions provided by the 4-MV Van de Graaff accelerator at the National Research Council of Canada was used to bombard evaporated targets of isotopically enriched ^{40}Ca deposited on 0.025-cm gold backings. Details of the targets and experimental techniques will be found in other publications.[4,5] In the region 9.3–9.6 MeV of excitation in ^{44}Ti, ten resonances have been observed using a NaI(Tl) detector to detect γ rays with energies between 6.5 and 7.5 MeV. On examination of the γ decay of these resonances using Ge(Li) detectors the likely candidate for the $T=2$ state was found at a ^{4}He energy of 4645 ± 5 keV by comparison with resonances previously studied.[4] A Ge(Li) γ-ray spectrum observed at 0° is shown in Fig. 1. The two most prominent γ rays have energies (at 90° to the beam direction) of 7215.4 ± 2.0 and 2122.0 ± 1.0 keV. Including nuclear recoil following γ-ray emission the sum of these two γ-ray energies places the resonance at 9338 ± 2 keV, in good agreement with the ^{4}He energy (using a Q value of 5118 ± 10 keV[4]) and with the location of the $T=2$ state as determined in the (p, t) work of Rapaport *et al.*[3]

In previous α-capture work[4] and in the (p, t) experiments[2,3] no level has been observed at 2122 keV. Furthermore, both γ rays show the full Doppler shift which in the case of the 2122-keV transition means that the lifetime of the emitting state is less than approximately 10^{-14} sec. A state at 2122 keV with such a lifetime would have to have spin 1 with an $E1$ enhancement of $\gtrsim 0.8\times10^{-2}$ W.u. [Weisskopf units] or an $M1$ enhancement $\gtrsim 0.3$ W.u. These would be unusually large for $\Delta T=0$ dipole transitions in a self-conjugate nucleus. The conclusion is that the γ-ray cascade from the resonance consists of the 2122-keV γ ray followed by the 7216-keV γ ray to the ground state.

The inset in Fig. 1 shows that the angular distributions of both γ rays are isotropic to within the statistical error. This is consistent with the lowest $T=2$ state having a J^π of 0^+ and with the $l=0$ angular distribution of the (p, t) reaction to the 9330-keV level.

The state at 7216 keV is likely a $T=1$ state of spin 1, because of the expected decay properties of $T=2$ states and because the experimental value of $\omega\gamma$ (see below) limits the 2122-keV radiation to dipole character. A state at 6600 ± 10 keV has been assigned in the (p, t) work of Rapaport *et al.*[3] as the $T=1$ analog of the 2^+ ground state of ^{44}Sc. The spin-1 state is thus 616 ± 10 keV above the $T=1$, 2^+ state. In ^{44}Sc there are two states near 600 keV and in particular a 1^+ state at 669 keV.[6,7] It is likely that the 7216-keV state is the analog